SYNTHESIS OBSERVATIONS OF SOUTHERN RADIO SOURCES AT 1410 MHz WITH THE PARKES INTERFEROMETER

I. INSTRUMENT, REDUCTION, AND PRELIMINARY RESULTS

By U. J. SCHWARZ,* D. J. COLE,† and D. MORRIS‡

[Manuscript received 13 March 1973]

Abstract

Modifications to the Parkes interferometer are described which allow synthesis observations to be made while still retaining the flexibility of frequent baseline changes. Details are given of the receiver with a phase stabilizing device and its performance, on-line computer control, and data processing. Preliminary observations with a resolution of 1′ of the two sources PKS 2152−69 and 2356−61 and possible optical identifications are discussed briefly.

I. INTRODUCTION

Earth rotation synthesis observations have been made with the Parkes interferometer on several southern sources, and the technique and results of preliminary observations of the unpolarized radiation of two of these sources are reported here. A subsequent paper in the series will describe measurements of the polarization.

The interferometer consisting of the Parkes 64 m telescope and an 18 m dish, which is movable on a north–south or east–west track, has been described by Cole (1967), Morris and Whiteoak (1968), and Batchelor *et al.* (1969). The minimum and maximum separations are 120 and 410 m respectively, and both dishes are altaz mounted. The interferometer was originally designed for continuous changes in antenna separation at the expense of limited phase stability and knowledge of the antenna position (to only about one wavelength at 1400 MHz). Although modifications of the system were introduced to overcome these limitations, it seemed desirable to retain the convenience of being able to readily change the length of the baseline. In this way the U–V plane available to the Parkes interferometer can be fully sampled in 12 hr, using the east–west baseline, for sources with $\delta < -67°$ (the 64 m telescope is restricted to zenith angles smaller than 60°). If both east–west and north–south baselines are used then it is possible to obtain reasonable coverage of the U–V plane for sources south of $\delta = -33°$.

* Sterrenkundig Laboratorium "Kapteyn", Rijksuniversiteit te Groningen, Postbus 800, Groningen, The Netherlands.

† Division of Radiophysics, CSIRO, P. O. Box 76, Epping, N.S.W. 2121.

‡ Division of Radiophysics, CSIRO; present address: Observatoire de Paris, 92-Meudon, France.

Aust. J. Phys., 1973, **26**, 661–73

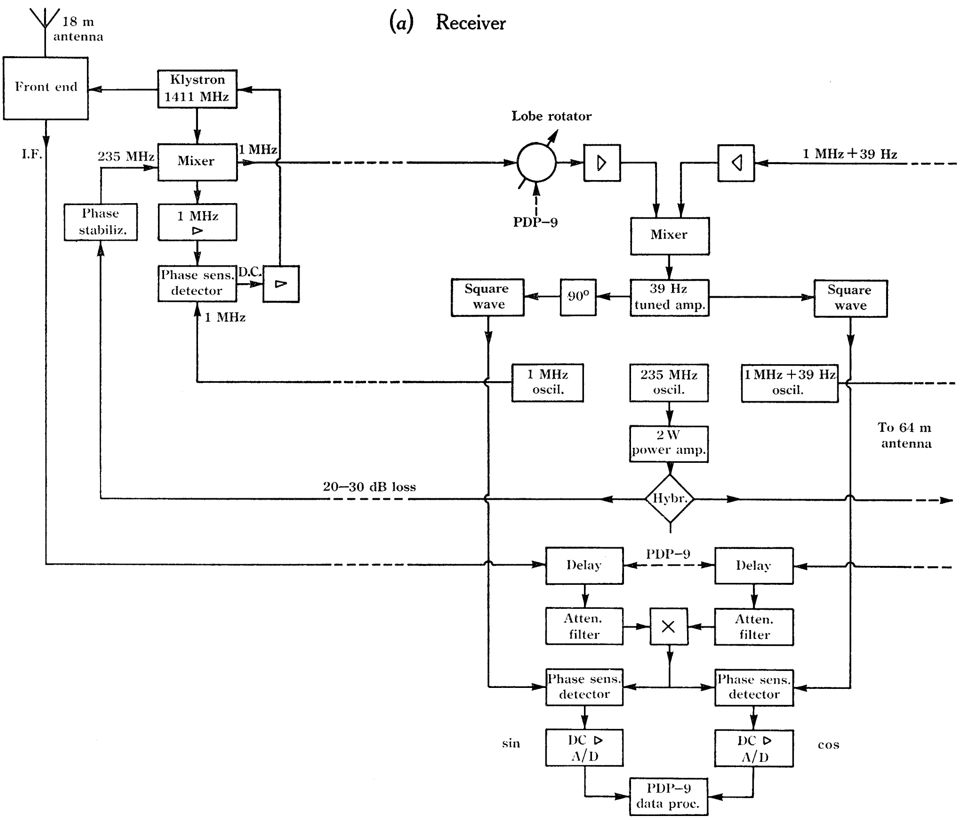

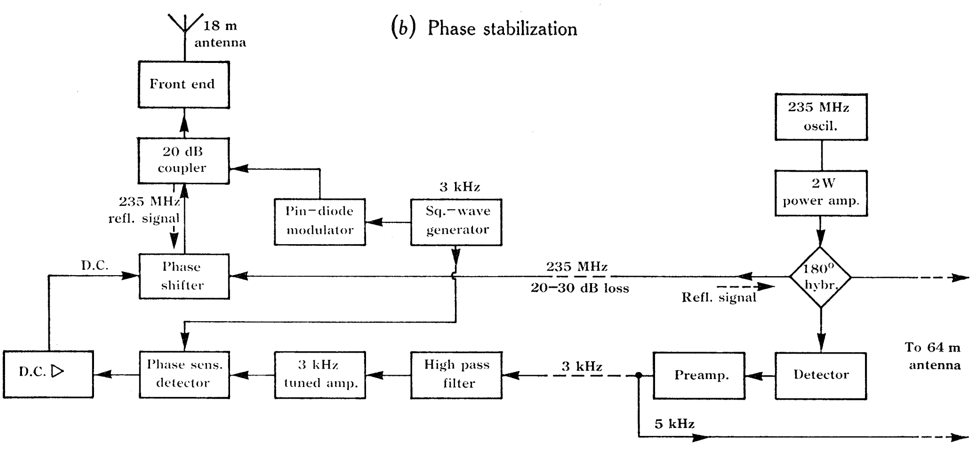

Fig. 1.—Block diagrams of the receiver and the phase-stabilizing system.

Several changes to the interferometer have been necessary for the present work:

(1) cosine and sine channels have been included;

(2) phase-stabilizing devices have been added to compensate for changes in the length of the local oscillator cables and for imperfections in the phase-locking circuits;

(3) digital computer control of the delays and the lobe rotator has been introduced;

(4) antenna position measurement has been improved.

Initially, frequent observations were made of a point calibration source located close to the region being synthesized. In this way a "relative" map could be constructed even with approximate antenna positions and slowly varying instrumental phase.

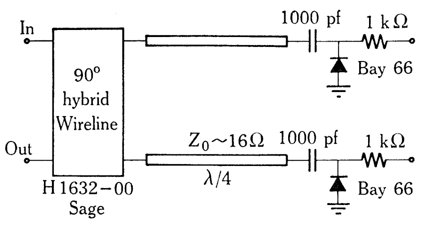

Fig. 2.—Details of the electrical phase shifter used in the phase-stabilizing system shown schematically in Figure 1(*b*).

II. Receiving System

Antennas and Feeds

Linearly polarized feeds were used: that for the 64 m telescope was a hybrid mode horn (Minnett and Thomas 1966) with two orthogonal probes, part of the signal from one probe being used (in conjunction with a line stretcher) to reduce the residual response to circular polarization; that for the 18 m telescope was a conical horn. Both receivers were provided with Micromega parametric amplifiers.

Sine and Cosine Channels

As described by Radhakrishnan *et al.* (1972), the interferometer was made compatible with the existing line receiver, which was designed for Dicke switching, by introducing a 39 Hz difference in the local oscillator frequencies at the two antennas. This difference frequency could be used to excite two phase-sensitive detectors in quadrature and thus obtain a sine component and a cosine component of the signal. A block diagram of the system is given in Figure 1(*a*). The local oscillator at each antenna was a klystron which was phase locked to the sixth harmonic of a 235 MHz signal, using a 1 MHz signal as reference.

Compensation for Phase-lock Errors

The 39 Hz reference for the phase-sensitive detectors was not derived directly from the 1 MHz oscillators, but from the 1 MHz beats of the klystron signals and the sixth harmonic of the 235 MHz signal. While this method was more complex, it made the instrumental phase of the interferometer insensitive to phase changes due to imperfections of the phase-lock loops.

Compensation for Line Length Changes

In principle the present arrangement is a Swarup circuit (Swarup and Yang 1961) extended into a servo system (Shimozawa 1968; R. S. Roger *et al.*, to be published), as shown schematically in Figure 1(*b*). An electrical phase shifter was used instead of a mechanical motor-driven device. The total loss of the cable connecting the two telescopes at 235 MHz was approximately 50 dB and was too high for the phase-lock system. The cable was therefore split at the midpoint of the track. Here the 235 MHz signal from a frequency synthesizer was amplified to a 2 W level and channelled into the two lines through a hybrid. As a consequence of this, the phase-stabilizing system had to be duplicated and two independent correcting systems were used, one for the local oscillator cable to each telescope. At the (antenna) end of each cable a fraction of the 235 MHz signal was reflected and modulated by a pin diode driven by a square-wave signal of 3 kHz at one antenna and 5 kHz at the other. The electrical phase shifter used a 90° hybrid and varactors (Fig. 2). By applying a potential of -1 to $+1$ V the phase of the 235 MHz signal could be changed by about 200°.

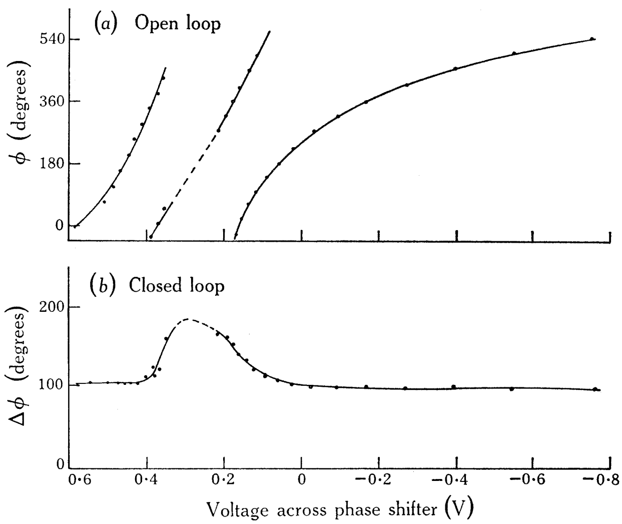

Fig. 3.—Results of the phase-stability test showing (*a*) the phase error ϕ introduced with change in length of the local oscillator cable and (*b*) the remaining observed phase change $\Delta\phi$ after correction by the servo system. The dashed parts of the curves are interpolated values from other similar observations. The zero points of the ϕ and $\Delta\phi$ scales are arbitrary.

The performance of the phase-stabilizing system depended, among other things, on the matching of the phase shifter and other inputs connected to the 235 MHz line which could cause secondary reflections. Since the matching of the phase shifter depended in turn on the applied d.c. voltage, a phase error could result and perfect compensation for changes in cable length might not be obtained. Figure 3 shows the results of a phase-stability test. It can be seen that the phase remained constant in the regions 0·4 to 0·6 and $-0{\cdot}8$ to 0 V across the phase shifter but changed by about

100° in the intermediate range 0 to 0·4 V. This latter range obviously had to be avoided for the observations. Some initial measurements were made in this interval, but since the phase-servo voltage was recorded for each it was possible to apply an approximate correction derived from data as plotted in Figure 3.

Interferometer Controls

The compensating delays were adjustable with a smallest step of 0·75 m. The lobe rotator operated on the 1 MHz beat frequency and was driven by a stepping motor, the smallest step normally used being 2°. It could be set to a zero position on pulse command. The logic and its realization have been described by Cole (1969).

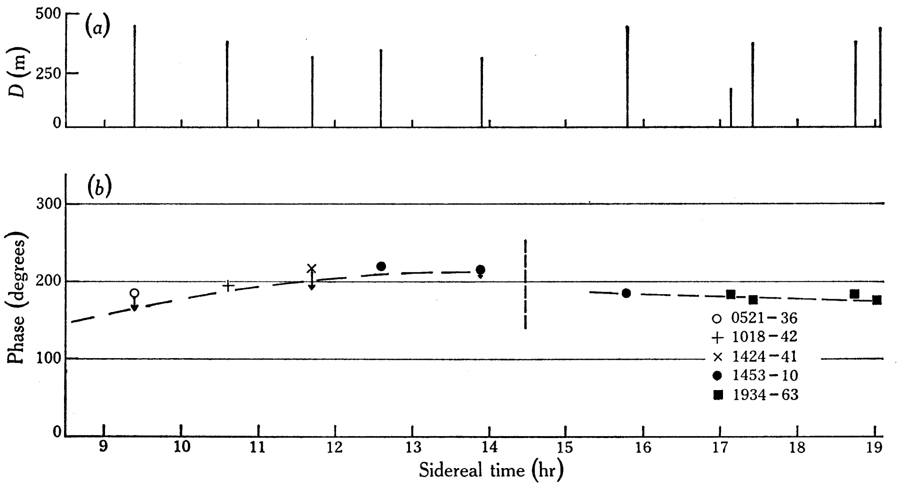

Fig. 4.—Example of a series of phase calibrations showing (*a*) the track distance D between the two antennas at which the observations of the indicated calibrating sources have been made and (*b*) the observed on-line computed phases. The arrows in (*b*) show subsequent corrections applied to certain measurements, as described in the text, while the dashed vertical line indicates the time of readjustment of the receiving system.

III. On-line Computer Control

The on-line computer had three functions:

(1) *Control of the interferometer.* The main function was to control the lobe rotator and the switching of the delays, and for this the path difference P was calculated. The instantaneous $(2\pi/\lambda)P$ phase was calculated every 20 ms and the lobe rotator up-dated if necessary to compensate for the Earth's motion. Similarly the delays were adjusted every 0·2 s. In order to make frequent changes in baseline length the 18 m telescope was moved by remote control and its position was compared automatically with surveyed reference markers as it passed over each of them. The accuracy was ± 3 mm.

(2) *Data collection.* The program had options for different predetermined sequences of integrations of the sine and cosine channels, controlling at the same time external devices such as the feed rotator.

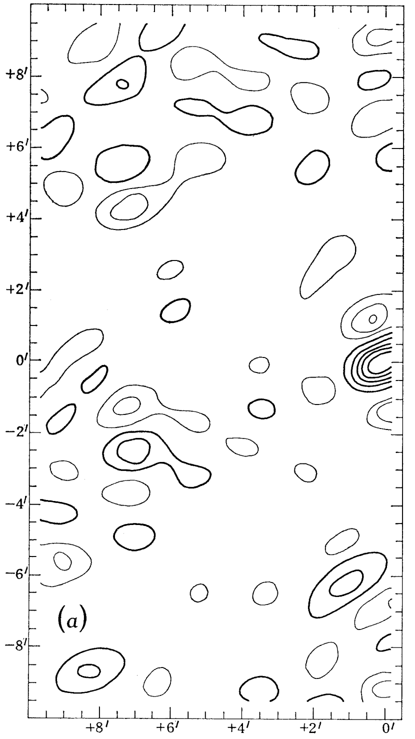

Figs. 5(*a*)–5(*d*).—Example of data processing using the iterative beam-removing technique. The effects of large side lobes are removed by transforming the source response into components of the beam pattern (*a*) and the corresponding brightness distribution (*b*) and then reconstructing the map using the central part of the beam only. The intermediate result (*c*) is after 10 iterations while the final result (*d*) is after 98 iterations. The dashed contours are spaced at double the contour interval elsewhere and light and bold contours indicate decreasing and increasing intensities respectively. The zero level has been omitted. Note the rotation of the coordinate system with respect to the frames of the maps.

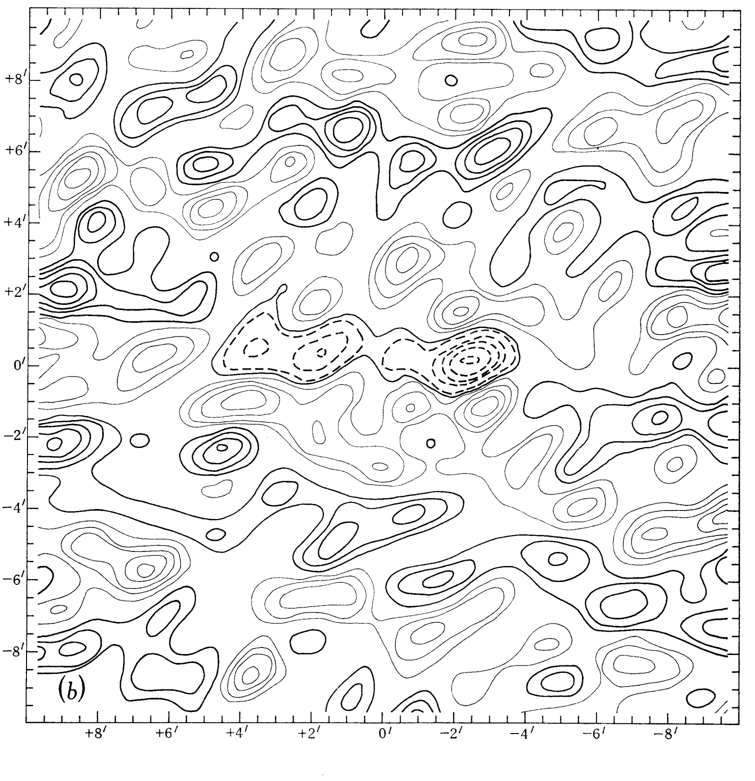

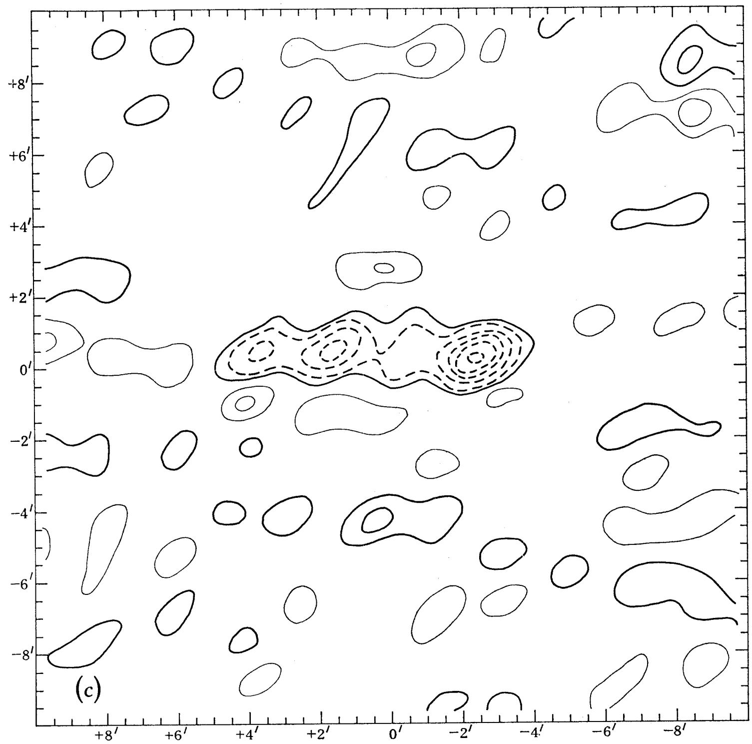
+8′
+6′
+4′
+2′
0′
−2′
−4′
−6′
−8′
(c)
+8′ +6′ +4′ +2′ 0′ −2′ −4′ −6′ −8′

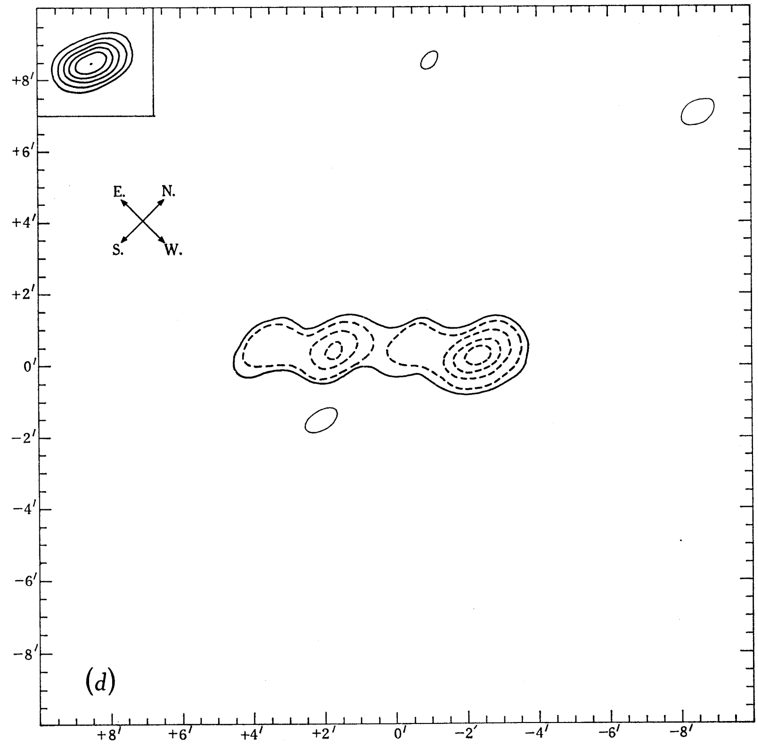
+8′
+6′
+4′
+2′
0′
−2′
−4′
−6′
−8′
E.
N.
S.
W.
(d)
+8′ +6′ +4′ +2′ 0′ −2′ −4′ −6′ −8′

(3) *Data processing after the observations.* The amplitude and phase of each integration, the average values, and the standard deviations were calculated. For the polarization measurements, observations could be made at a series of position angles and first and second harmonics were fitted to the integration of each channel. This then gave amplitude and position angle of the linearly polarized components (a correction for the parallactic angle was included).

IV. Method of Observation and Performance of System

Several extended sources of 10′ or less, for which a sampling interval of 66 m in the *U–V* plane was needed, were selected from the work of Ekers (1969*b*). Observations were made by starting at the maximum spacing (410 m) at an hour angle of −6 hr and making consecutive observations as the baseline was reduced in 61 m decrements to a minimum of 128 m. Such a series of observations took about an hour and corresponded to a movement of the telescope in the *U–V* plane of 100 m maximum in the *U* direction. This sequence was repeated during a 12 hr period (making fewer observations at lower spacings) to obtain a reasonably uniform distribution of observations across the *U–V* plane.

In the initial observations of the two sources considered here, a calibrator was observed at each setting of the 18 m telescope to adjust the phase and amplitude readings. However, this procedure was later found to be unnecessary, since the distance determination was sufficiently accurate and the instrumental phase stayed constant even though the telescope had been moved, and subsequently a calibrator was measured only once an hour. An example of a series of calibrations over a 9 hr period is given in Figure 4. Some calibrations had to be corrected for a phase shift introduced by the phase-servo system (see Section II); such corrections are indicated by arrows in the figure.

All observations after the initial stage were adjusted in phase and amplitude using a smooth function in time derived from the calibration measurements. The r.m.s. errors were estimated to be 3% in amplitude and 6% in phase. Accurate *U* and *V* coordinates were also calculated for the midpoint of the start and end time of each observation. Values with large internal standard deviations (see Section III) were disregarded.

V. Fourier Inversion

Instead of the usual approach of interpolating the visibility function into a regular grid, a different method was used here because of the fact that the *U–V* plane was sampled only sufficiently for spacings greater than 128 m (600λ) and a far-reaching interpolation would have been necessary to fill this large gap. The alternative method, which is especially suited for incomplete coverage of data, has been developed by J. A. Högbom (to be published) and applied by Rogstad and Shostak (1971). It is an iterative beam-removing technique in which the effects of large side lobes are eliminated by splitting the beam response into its components and then restoring the map from the central, or "clean", component of the beam only.

An example of the data processing technique is given in Figures 5(*a*)–5(*d*), which illustrate the transformed beam pattern, the uncorrected brightness distribution, an intermediate stage in the iterative procedure, and the final result after 98 iterations. A theoretical foundation for this technique is not yet available, and our approach was an empirical one in that several tests were made to see under which conditions the iterations converged and if a unique solution was always obtained. The method appeared to give useful results under all conditions encountered in the present observations.

No zero spacing value is needed to apply the iterative method and the integrated flux is determined as a by-product, independent of single-dish observations. The final results presented in the following section were obtained for both sources after 98 iterations. The central processor time on the CDC 6600 computer was approximately 20 s for a grid of 40×40 points.

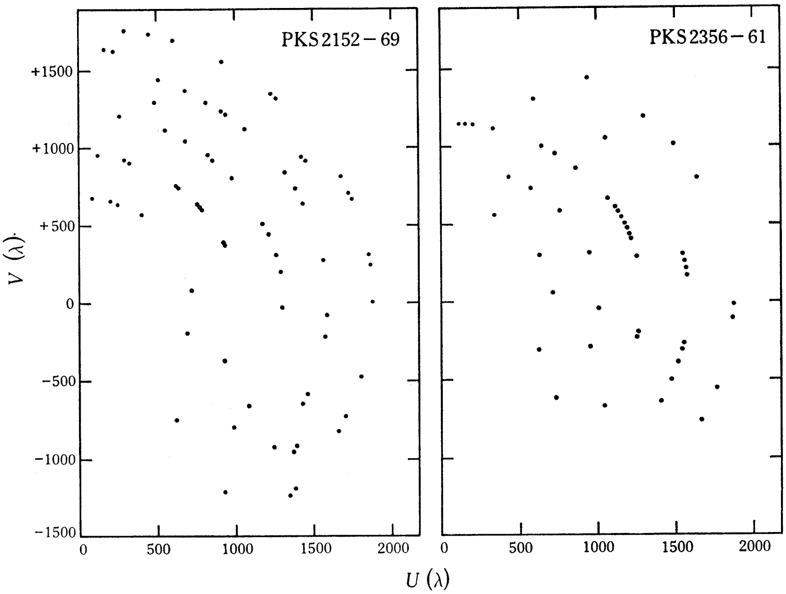

Fig. 6.—*U–V* coverage of the two sources observed.

VI. Results

The sources PKS 2152−69 and 2356−61 have been observed using as calibrators for phase and amplitude the point sources PKS 1934−63 and 2331−41 respectively. The accurate position of an optical identification of PKS 1934−63 (Sutton 1968) has been assumed, while PKS 2331−41 has been taken to have an uncertainty in position of not larger than 15″ (Shimmins *et al.* 1966). However, when the calibration based on PKS 1934−63 was used to derive a position for PKS 2331−41 from the present observations, this position agreed with that of Shimmins *et al.* to within 4″, and hence the absolute position calibration of the map of PKS 2356−61 is probably good to this accuracy also.

For these preliminary observations, no polarization measurements were attempted and the feed polarization angle was kept fixed with respect to the antennas.

Hence, no allowance for the changing parallactic angle has been made and the resulting maps refer approximately to the total intensity, since neither source is strongly polarized. The *U–V* coverage of both sources is shown in Figure 6, while the resulting maps after processing are presented in Figures 7 and 8, together with the synthesized processed beams. Although only a small area is included around the source in each map, square fields of 16′ and 20′ width respectively were used for the transformation and processing of the data in Figures 7 and 8 and spurious responses did not reach the value of the second lowest contour.

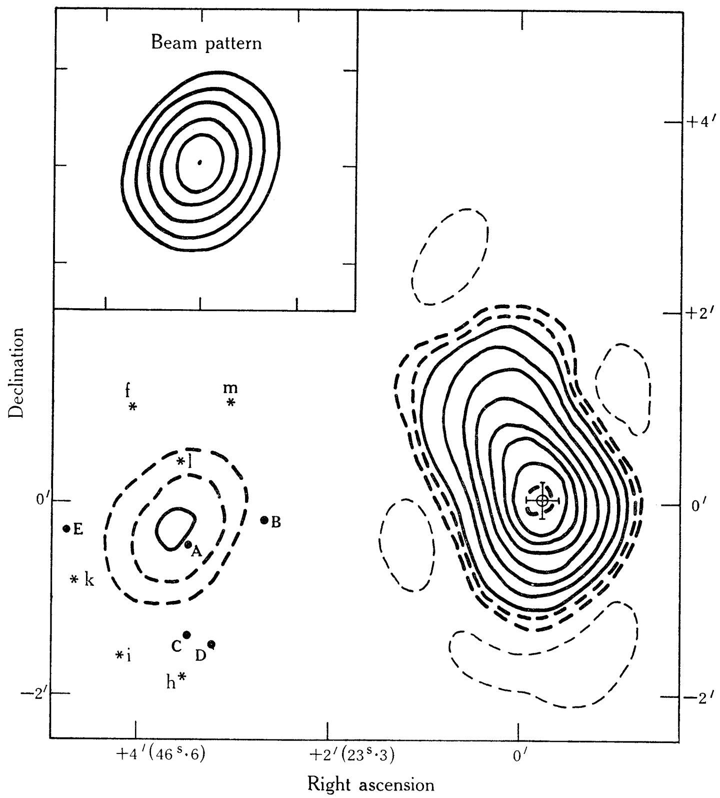

Fig. 7.—Resulting map of the source PKS 2152−69. The first dashed contour is at 80 K and the interval between the dashed contours is 80 K while that between the continuous contours is 240 K. The cross indicates the position of the galaxy identified by Westerlund and Smith (1966). The points A–E show the positions of five other optical objects and the asterisks give the locations of reference stars. The origin of the map is at R.A.(1950·0) $21^h 53^m 00^s$, Dec.(1950·0) $-69° 55' 46''$.

PKS 2152−69

The resolution of this source into an extended major component with an unresolved weaker companion is in agreement with the results of Sutton (1968) and Ekers (1969*b*). In the present case, however, a more accurate declination can also be given. The positions of the first moments of the main and secondary components were found to be:

	Right ascension (1950·0)	Declination (1950·0)
Main component	$21^h 52^m 59^s \pm 1^s$ ($58^s{\cdot}5 \pm 0^s{\cdot}11$)	$-69° 55' 27'' \pm 3''$
Galaxy	$21^h 52^m 57^s{\cdot}8$	$-69° 55' 40''{\cdot}2$
Secondary component	$21^h 53^m 41^s \pm 2^s$ ($38^s{\cdot}1 \pm 0^s{\cdot}3$)	$-69° 56' 02'' \pm 5''$
Faint image	$21^h 53^m 40^s{\cdot}5 \pm 0^s{\cdot}2$	$-69° 56' 11''{\cdot}2 \pm 1''{\cdot}0$

The values in parentheses are those measured by Sutton (1968).

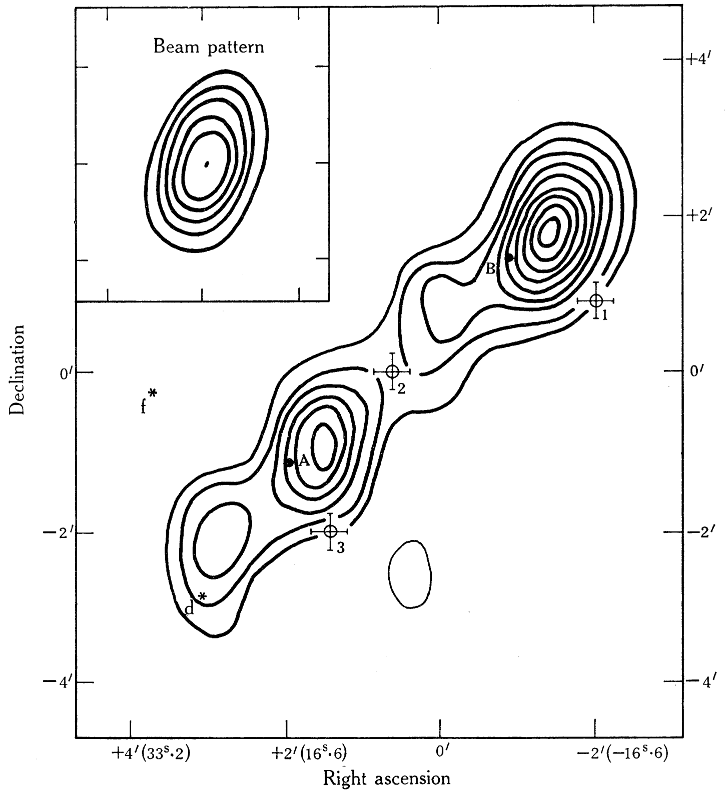

Fig. 8.—Resulting map of the source PKS 2356−61. The contour interval and the level of the first contour is 220 K. The crosses indicate the positions of three galaxies given by Westerlund and Smith (1966), while A and B are two other optical objects, of which B is probably a galaxy. The asterisks d and f give the locations of reference stars. The origin of the map is at R.A.(1950·0) $23^h 56^m 24^s{\cdot}3$, Dec.(1950·0) $-61° 11' 40''$.

The optical identification of the only galaxy mentioned by Westerlund and Smith (1966) is confirmed (see Fig. 7). A contact print of a 74 in. plate from Mt. Stromlo has been searched for an optical counterpart of the secondary source and the only possible identification found is a faint image of about 20–21 magnitude, whose optical position as listed above is marked A in Figure 7. Although its position agrees in right ascension with the present measurements and to within 2σ in declination, the disagreement in right ascension with the measurement of Sutton (1968) is 6σ. The positions of four other similar objects (B, C, D, and E) are also marked in Figure 7, while the asterisks indicate reference stars, that labelled f being the star used by Westerlund and Smith.

There is a difference in spectral index between the two components of the source, as noted by Ekers (1969*b*) from a comparison of the 1410 and 408 MHz flux densities. The secondary source has a steeper spectrum, with a spectral index $\alpha \leqslant -0\cdot 88$ as opposed to $-0\cdot 66$ for the extended component (α being defined here by $S_\nu \propto \nu^\alpha$, with S_ν the flux density at frequency ν). This may indicate an identification with a radio galaxy. The difference in spectral index is even more apparent when the integrated flux densities of the main component, rather than the peak intensities, are used at both frequencies. The present value of the integrated flux density is found to be 23·0 f.u., somewhat smaller than the 1410 MHz value of 25·9 f.u. given in the Parkes catalogue Ekers (1969*a*).

PKS 2356−61

The crosses in Figure 8 mark the positions of the prominent galaxies noted by Westerlund and Smith (1966). The identification (galaxy 2) lies on the major axis of the radio source close to the midpoint. Inspection of a contact print of a 74 in. plate from Mt. Stromlo revealed two other faint objects, marked A and B in the figure, both of magnitudes between 19 and 21. The object B looks somewhat extended and is probably a galaxy. Two of the reference stars (d and f) used by Westerlund and Smith are also included in the figure. In general the synthesized map agrees with the results of the model-fitting procedure used by Ekers (1969*b*), although the source is not as symmetrical as was suggested by the model. This asymmetry is also confirmed by strip scans carried out by J. M. Sutton (personal communication). The present value for the integrated flux density is 19·3 f.u. (the Parkes catalogue gives 19·2 f.u.).

VII. Acknowledgments

The observations were made during a visit by one of us (U.J.S.) to the Division of Radiophysics, CSIRO. We primarily acknowledge the assistance given to us by the staff of the observatory at Parkes during the observations, especially Mr. L. F. Fellows, and also the help of Mr. B. F. C. Cooper, Mr. J. W. Brooks, Mr. J. D. Murray, Mr. V. Radhakrishnan, and Dr. J. B. Whiteoak among others at the Division. The reduction of the observations was mostly performed on a CDC 6600 at the Computing Centre of the University of Groningen, partly using programs compiled by Dr. D. H. Rogstad. We also thank Dr. R. D. Ekers for many discussions, Mr. E. R. R. Timmerman for the preparation of the figures, Dr. B. J. Robinson for a critical reading of the manuscript, and Mr. N. R. Stokes for the contact copies of the 74 in. plates from Mt. Stromlo.

VIII. References

Batchelor, R. A., Cooper, B. F. C., Cole, D. J., and Shimmins, A. J. (1969).—*Proc. IREE Aust.* **30**, 305.

Cole, D. J. (1967).—*Proc. astr. Soc. Aust.* **1**, 30.

Cole, D. J. (1969).—*Proc. IREE Aust.* **30**, 153.

Ekers, Jennifer A. (Ed.) (1969*a*).—*Aust. J. Phys. astrophys. Suppl.* No. 7.

Ekers, R. D. (1969*b*).—*Aust. J. Phys. astrophys. Suppl.* No. 6.
Minnett, H. C., and Thomas, B. McA. (1966).—*IEEE Trans. Antennas Propag.* AP **14**, 654.
Morris, D., and Whiteoak, J. B. (1968).—*Aust. J. Phys.* **21**, 475.
Radhakrishnan, V., Brooks, J. W., Goss, W. M., Murray, J. D., and Schwarz, U. J. (1972).—*Astrophys. J. Suppl. Ser.* **24**, 1.
Rogstad, D. H., and Shostak, G. S. (1971).—*Astr. Astrophys.* **13**, 99.
Shimmins, A. J., Clarke, Margaret E., and Ekers, R. D. (1966).—*Aust. J. Phys.* **19**, 649.
Shimozawa, D. T. (1968).—M.A.Sc. Thesis, University of British Columbia.
Sutton, J. M. (1968).—*Aust. J. Phys.* **21**, 221.
Swarup, G., and Yang, K. S. (1961).—*I.R.E. Trans. Antennas Propag.* AP **9**, No. 1.
Westerlund, B. E., and Smith, L. F. (1966).—*Aust. J. Phys.* **19**, 181.